CORA Cork Open Research Archive
Cartlann Taighde Oscailte Chorcaí

Title	Modeling the capacitance-voltage response of In0.53Ga0.47As metal-oxide-semiconductor structures: Charge quantization and nonparabolic corrections
Author(s)	O'Regan, Terrance P.; Hurley, Paul K.; Sorée, Bart; Fischetti, Massimo V.
Publication date	2010
Original citation	O'Regan, T. P., Hurley, P. K., Sorée, B. and Fischetti, M. V. (2010) 'Modeling the capacitance-voltage response of In0.53Ga0.47As metal-oxide-semiconductor structures: Charge quantization and nonparabolic corrections', Applied Physics Letters, 96(21), pp. 213514. doi: 10.1063/1.3436645
Type of publication	Article (peer-reviewed)
Link to publisher's version	http://aip.scitation.org/doi/abs/10.1063/1.3436645 http://dx.doi.org/10.1063/1.3436645 Access to the full text of the published version may require a subscription.
Rights	**© 2010 American Institute of Physics.This article may be downloaded for personal use only. Any other use requires prior permission of the author and AIP Publishing. The following article appeared in O'Regan, T. P., Hurley, P. K., Sorée, B. and Fischetti, M. V. (2010) 'Modeling the capacitance-voltage response of In0.53Ga0.47As metal-oxide-semiconductor structures: Charge quantization and nonparabolic corrections', Applied Physics Letters, 96(21), pp. 213514 and may be found at http://aip.scitation.org/doi/abs/10.1063/1.3436645**
Item downloaded from	http://hdl.handle.net/10468/4341

Downloaded on 2019-01-22T01:45:04Z

UCC
University College Cork, Ireland
Coláiste na hOllscoile Corcaigh

Modeling the capacitance-voltage response of $In_{0.53}Ga_{0.47}As$ metal-oxide-semiconductor structures: Charge quantization and nonparabolic corrections

T. P. O'Regan' , P. K. Hurley, B. Sorée, and M. V. Fischetti

Citation: Appl. Phys. Lett. **96**, 213514 (2010); doi: 10.1063/1.3436645
View online: http://dx.doi.org/10.1063/1.3436645
View Table of Contents: http://aip.scitation.org/toc/apl/96/21
Published by the American Institute of Physics

Articles you may be interested in

1-nm-capacitance-equivalent-thickness HfO_2/Al_2O_3/InGaAs metal-oxide-semiconductor structure with low interface trap density and low gate leakage current density
Applied Physics Letters **100**, 132906 (2012); 10.1063/1.3698095

Band parameters for III–V compound semiconductors and their alloys
Journal of Applied Physics **89**, 5815 (2001); 10.1063/1.1368156

Modeling the capacitance-voltage response of $In_{0.53}Ga_{0.47}As$ metal-oxide-semiconductor structures: Charge quantization and nonparabolic corrections

T. P. O'Regan,[1,a)] P. K. Hurley,[1] B. Sorée,[2] and M. V. Fischetti[3]
[1]*Tyndall National Institute, University College Cork, Lee Maltings, Prospect Row, Cork, Ireland*
[2]*Interuniversity Microelectronics Center (IMEC vzw), Kapeldreef 75, B-3001 Leuven, Belgium*
[3]*University of Massachusetts Amherst, 100 Natural Resources Road, Amherst, Massachusetts 01003, USA*

(Received 24 March 2010; accepted 6 May 2010; published online 27 May 2010)

The capacitance-voltage (*C-V*) characteristic is calculated for p-type $In_{0.53}Ga_{0.47}As$ metal-oxide-semiconductor (MOS) structures based on a self-consistent Poisson–Schrödinger solution. For strong inversion, charge quantization leads to occupation of the satellite valleys which appears as a sharp increase in the capacitance toward the oxide capacitance. The results indicate that the charge quantization, even in the absence of interface defects (D_{it}), is a contributing factor to the experimental observation of an almost symmetric *C-V* response for $In_{0.53}Ga_{0.47}As$ MOS structures. In addition, nonparabolic corrections are shown to enhance the depopulation of the Γ valley, shifting the capacitance increase to lower inversion charge densities. © *2010 American Institute of Physics*.
[doi:10.1063/1.3436645]

High bulk-mobility III-V semiconductors, such as $In_{0.53}Ga_{0.47}As$ (simply InGaAs from here on), have recently garnered attention[1] as a potential solution to metal-oxide-semiconductor (MOS) transistor-scaling beyond the minimum feature size of 22 nm.[2,3] As a consequence, it is important to understand the theoretical variation in surface charge density and capacitance as a function of voltage in InGaAs MOS systems. In addition, practical InGaAs MOS structures exhibit a high density (typically $>10^{12}$ cm^{-2}) of interface states, which will degrade the subthreshold slope in InGaAs MOS field-effect-transistors (MOSFETs).[4–6] The characterization of D_{it} in InGaAs MOS systems is based on an analysis of the measured capacitance or conductance of the MOS structure as a function of applied bias. An analysis of interface states from capacitance is based on the deviation of the measured capacitance-voltage (*C-V*) response from the ideal *C-V*, and as a consequence, the calculation of the ideal *C-V* response is of interest from both a theoretical perspective and for the calculation of D_{it} levels for InGaAs MOS structures.

Due to the low density-of-states (DOS) in the InGaAs Γ valley, the theoretical *C-V* characteristics of InGaAs MOS systems can exhibit an asymmetric response, with a reduced capacitance as the Fermi level enters the conduction band.[7] The results reported in Ref. 7 employed a classical approach, and did not include charge quantization or nonparabolic corrections. Generally, the Γ valley of III-V semiconductors exhibits a small effective-mass and strong nonparabolicity.[8,9] The "heavier" satellite valleys can play an important role, especially under strong quantization,[10] making it necessary to include charge quantization and nonparabolic corrections to more accurately model the valley occupations and corresponding *C-V* characteristics. In this work we extend the results presented in Ref. 7 to include charge quantization and nonparabolic corrections, as well as including the effect of the occupancy of the X and L satellite valleys on the *C-V* response.

The calculation[11] consists of the numerical solution to the Schrödinger equation, as follows:

$$\left[-\frac{\hbar^2}{2m_x}\frac{d^2}{dx^2}+V(x)\right]\zeta_\nu(x)=E_\nu\zeta_\nu(x), \quad (1)$$

where E_ν and ζ_ν are the energy subband minima and envelope wave functions in subband ν, and m_x is the effective mass along the direction of quantization. The effective potential energy is $V(x)=-e\psi(x)+V_{im}(x)+V_{xc}(x)$, where $-e\psi(x)$ is the potential energy, $V_{im}(x)$ is the image potential[12] and $V_{xc}(x)$ is the exchange-correlation energy.[13,14] Equation (1) is solved self-consistently with Poisson's equation, as follows:

$$\frac{d^2\psi(x)}{dx^2}=-\frac{e}{\epsilon_s}[p(x)-n_{qm}(x)-N_a], \quad (2)$$

where ϵ_s is the semiconductor dielectric constant, $p(x)$ is the classical hole density calculated with Fermi–Dirac statistics, and N_a is the constant p-type doping. The quantum mechanical electron-density is calculated as follows:[15,16]

$$n_{qm}(x)=\frac{kT}{\pi\hbar^2}\sum_\mu g_\mu m_{d,\mu}\{[1+2\alpha(E_\mu-U_\mu)]F_0(\eta)+2\alpha kTF_1(\eta)\}|\zeta_\mu(x)|^2, \quad (3)$$

where $F_0(\eta)$ and $F_1(\eta)$ are the Fermi–Dirac integrals of order 0 and 1, $\eta=(E_F-E_\mu)/kT$, U_μ is the expectation value of the potential energy,[16] α is the nonparabolicity parameter,[15,16] g_μ and $m_{d,\mu}$ are the degeneracy and DOS effective mass in subband μ, T is the temperature, and E_F is the Fermi level. For comparison, the *C-V* response is also calculated using the classical electron density, $n(x)$, with Fermi–Dirac statistics. Note that Eqs. (1) and (3) have implicit valley and ladder indices when including the oblong X and L valleys.

From Gauss's law, the net sheet-charge in the semiconductor is $Q_s=-\epsilon_sE_s$, where E_s the electrical field at the semiconductor surface. The semiconductor capacitance is then

a)Electronic mail: terrance.oregan@tyndall.ie.

 © 2010 American Institute of Physics

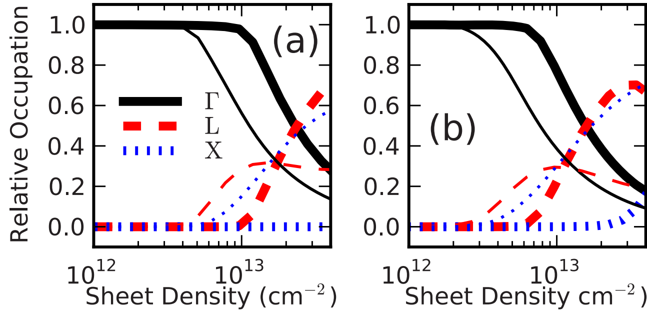

FIG. 1. (Color online) Relative valley occupations vs electron sheet density for parabolic bands (a) and with nonparabolic corrections (b). The thick lines are for $E_\Gamma = 0.73$ eV, $E_L = 1.49$ eV, $E_X = 1.98$ eV (MVF, unpublished), and the thin lines are for $E_\Gamma = 0.74$ eV, $E_L = 1.2$ eV, and $E_X = 1.33$ eV (Ref. 17).

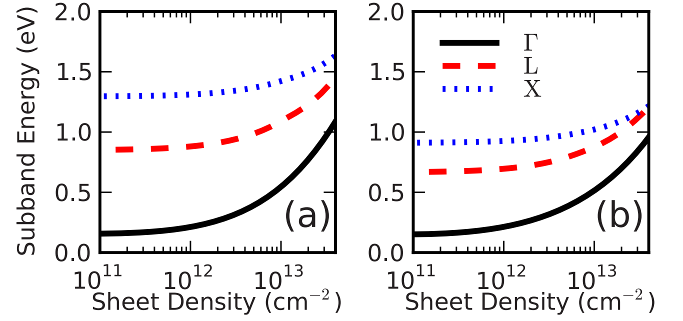

FIG. 2. (Color online) Energy subband minima vs electron sheet density for parabolic bands (a), and with nonparabolic corrections (b). The energies of the lowest subband in each valley are shown and are referenced to the lowest conduction band at the oxide/semiconductor interface, $E_c|_{x=0}$.

calculated as $C_s(\psi_s) = dQ_s/d\psi_s$, where Q_s depends implicitly on the surface potential, ψ_s, and the total MOS capacitance is, as follows:

$$\frac{1}{C_{tot}} = \frac{1}{C_{ox}} + \frac{1}{C_s + C_{it}}, \tag{4}$$

where $C_{ox} = \epsilon_{ox}/t_{ox}$ is the oxide capacitance, ϵ_{ox} is the oxide dielectric constant, and t_{ox} is the physical oxide thickness. The interface-trap capacitance is: $C_{it}(\psi_s) = dQ_{it}/d\psi_s$, where the interface-trap density in Fig. (4) of Ref. 7 is used in Fig. 4 to calculate the interface sheet charge, Q_{it}, at the dielectric/semiconductor interface. Now the gate voltage can be written as: $V_G = \psi_s + \phi_{ms} - Q_s/C_{ox} - Q_{it}/C_{ox}$, where $\phi_{ms} = \phi_m - \phi_s$ is the difference between the metal and semiconductor workfunctions.

The device parameters used in this work are $N_a = 2 \times 10^{17}$ cm^{-3}, the gate dielectric is 2 nm of Al_2O_3 with $\epsilon_s = 9\epsilon_0$ ($t_{ox} = 10$ nm is also used in Fig. 3), and the metal workfunction is set to 5.05 eV. The literature reveals a wide range for the energy separations between the top of the valence band and the satellite-valley-minima. For instance, Ref. 17 suggests $E_L = 1.2$ eV and $E_X = 1.33$ eV, Ref. 9 suggests $E_L = 1.3713$ eV and $E_X = 1.3422$ eV, Ref. 18 calculates $E_L = 1.29$ eV and $E_X = 1.78$ eV, and an unpublished pseudopotential calculation performed by one of us (M.V. Fischetti) finds $E_L = 1.49$ eV and $E_X = 1.98$ eV. In this paper we use the extreme values ($E_L = 1.49$ eV, $E_X = 1.98$ eV and $E_L = 1.2$ eV, $E_X = 1.33$ eV) to explore the entire range in the literature. The nonparabolicity parameter used in the Γ valley, $\alpha_\Gamma = 1$ eV^{-1}, is a compromise between the almost parabolic behavior seen for m_x along the (100) confinement direction, and the nonparabolic behavior seen for the DOS-effective-mass in two-dimensional. Because of a lack of data, the Si nonparabolicity parameters[15,16] are used for the satellite valleys, $\alpha_L = \alpha_X = 0.5$ eV^{-1}.

Figure 1 shows the valley occupation (sum over all subband occupations within each valley) as a function of the electron sheet density, n_s, in the channel. As n_s increases in Fig. 1(a), the satellite valleys become occupied as the lighter mass Γ-valley is more strongly quantized, shown in Fig. 2(a) for the parabolic case. Figure 1(b) shows that including nonparabolic corrections further exasperates this trend, pushing the occupation of the satellite valley to smaller n_s, because the strong nonparabolic correction in the Γ valley results in a narrowing of the energy-level spacing, shown in Fig. 2(b). Figure 1 also shows that satellite-valley occupation (thin lines) shifts to lower n_s when using $E_L = 1.2$ eV and $E_X = 1.33$ eV.

For reference, Figs. 3(a) and 3(b) show the electron sheet density as a function of gate voltage for $t_{ox} = 2$ nm and $t_{ox} = 10$ nm, respectively. Figure 3(c), $t_{ox} = 2$ nm, illustrates the impact of the subband occupancy and nonparabolic bands on the resulting *C-V* response for the case of the Γ valley only and for the inclusion of the X and L valleys with parabolic and nonparabolic bands. To highlight the region of interest, the *C-V* response is shown from the onset of strong inversion. From the figure, the inclusion of the satellite valleys results in a marked increase ("shoulder") in the capacitance (1.5 V, $n_s = 6 \times 10^{12}$ cm^{-2} for $E_L = 1.49$ eV, $E_X = 1.98$ eV and 1.1 V, $n_s = 3 \times 10^{12}$ cm^{-2} for $E_L = 1.2$ eV, $E_X = 1.33$ eV) as the occupancy of the L valleys becomes significant. Moreover, the increase in the capacitance is shifted to lower gate voltages when nonparabolic corrections

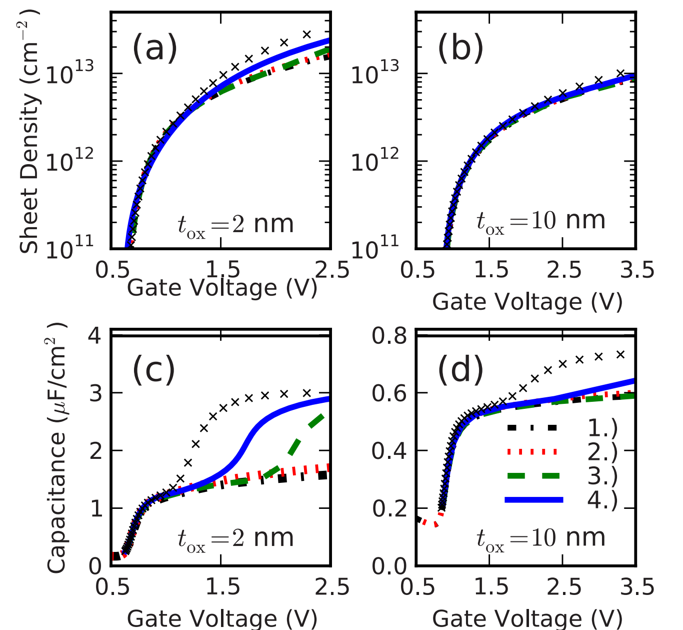

FIG. 3. (Color online) Electron sheet density vs gate voltage for $t_{ox} = 2$ nm (a) and $t_{ox} = 10$ nm (b). Total capacitance ($D_{it} = 0$) for $t_{ox} = 2$ nm (c) and $t_{ox} = 10$ nm (d). The four cases are: (1) parabolic Γ valley only, (2) Γ valley with nonparabolic corrections, (3) all valleys assuming parabolic bands, and (4) all valleys with nonparabolic corrections. Note that $E_L = 1.49$ eV and $E_X = 1.98$ eV except for the symbols which are case (4) with $E_L = 1.2$ eV and $E_X = 1.33$ eV. The horizontal lines in (c) and (d) are C_{ox}.

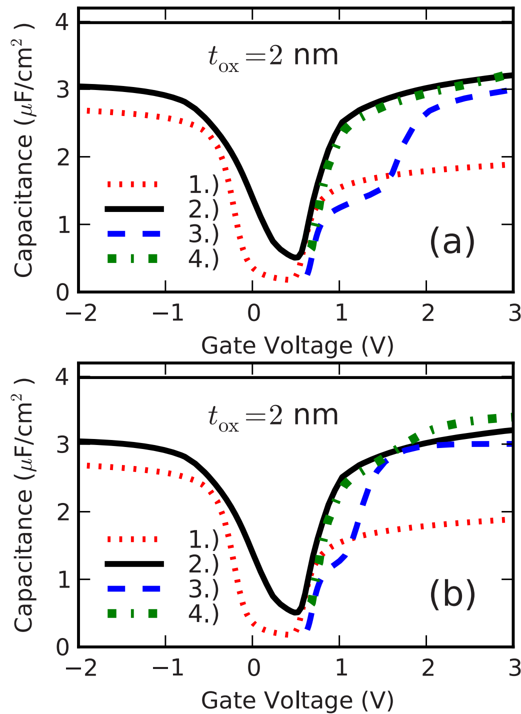

FIG. 4. (Color online) Total capacitance using $E_L=1.49$ eV and $E_X=1.98$ eV (a), and using $E_L=1.2$ eV and $E_X=1.33$ eV (b). The four cases are: (1) classical without D_{it}, (2) classical with D_{it}, (3) all valleys with nonparabolic corrections without D_{it}, and (4) all valleys with nonparabolic corrections with D_{it}. The horizontal lines are C_{ox}.

are included, corresponding to the results shown in Fig. 1. Figure 3(d) is the same as Fig. 3(c) except $t_{ox}=10$ nm. In this case the onset of the shoulder is visible for $E_L=1.49$ eV and $E_X=1.98$ eV but is pronounced for $E_L=1.2$ eV and $E_X=1.33$ eV.

Figure 4 shows the full *C-V* characteristics with and without a D_{it} profile across the InGaAs energy gap. In Fig. 4 we see that interface states alone, without charge quantization included, can explain the symmetric *C-V* characteristics, as presented in Ref. 7. The shoulder in the capacitance and subsequent increase toward C_{ox}, which appears when including charge quantization, is completely masked by the C_{it} contribution. We note here that the same D_{it} distribution in Ref. 7 is used here, while in reality the distributions are most likely dependent on oxide thickness and growth conditions. We notice that the capacitance shoulder is shifted to lower gate voltages in Fig. 4(b). This shift is a direct result of the occupation of the satellite valleys (especially the X valley) which is strongly dependent on E_L and E_X as shown in Fig. 1.

In conclusion, we have shown that including charge quantization and nonparabolic corrections in p-$In_{0.53}Ga_{0.47}As$ MOS structures results in the occupation of the satellite valleys and an associated increase in capacitance for channel electron-densities in the range $n_s=3-6\times10^{12}$ cm^{-2} depending on E_L and E_X. Conclusive agreement in the literature for the bandstructure of $In_{0.53}Ga_{0.53}As$ is needed so that quantitative comparisons to experimental *C-V* characteristics can be made. This effect could be a contributing factor to the symmetric-maximum capacitance generally observed for n- and p-doped InGaAs MOS structures. This work suggests the emergence of interesting *C-V* features for InGaAs MOS structures if D_{it} can be reduced.

This research was supported by the Science Foundation Ireland through the U.S.-Ireland Research Project (Project No. 08/U.S./I1546). Part of this work was conducted by TOR at University of Massachusetts Amherst and at IMEC.

[1] N. Goel, P. Majhi, C. O. Chui, W. Tsai, D. Choi, and J. S. Harris, Appl. Phys. Lett. **89**, 163517 (2006).
[2] W. Haensch, E. J. Nowak, R. H. Dennard, P. M. Solomon, A. Bryant, O. H. Dokumaci, A. Kumar, X. Wang, J. B. Johnson, and M. V. Fischetti, IBM J. Res. Dev. **50**, 339 (2006).
[3] M. Wistey, U. Singisetti, G. Burek, E. Kim, B. J. Thibeault, A. Nelson, J. Cagnon, Y.-J. Lee, S. R. Bank, S. Stemmer, P. C. McIntyre, A. C. Gossard, and M. J. Rodwell, ECS Trans. **19**(5), 361 (2009).
[4] W. E. Spicer, P. W. Chye, P. R. Skeath, C. Y. Su, and I. Lindau, J. Vac. Sci. Technol. **16**, 1422 (1979).
[5] M. Hong, J. R. Kwo, P.-c. Tsai, Y. Chang, M.-L. Huang, C.-p. Chen, and T.-d. Lin, Jpn. J. Appl. Phys. **46**, 3167 (2006).
[6] E. O'Connor, S. Monaghan, R. D. Long, A. O'Mahony, I. M. Povey, K. Cherkaoui, M. E. Pemble, G. Brammertz, M. Heyns, S. B. Newcomb, V. V. Afanas'ev, and P. K. Hurley, Appl. Phys. Lett. **94**, 102902 (2009).
[7] G. Brammertz, H.-C. Lin, M. Caymax, M. Meuris, M. Heyns, and M. Passlack, Appl. Phys. Lett. **95**, 202109 (2009).
[8] E. O. Kane, J. Phys. Chem. Solids **1**, 249 (1957).
[9] I. Vurgaftman, J. R. Meyer, and L. R. Ram-Mohan, J. Appl. Phys. **89**, 5815 (2001).
[10] A. Pethe, T. Krishnamohan, D. Kim, O. Oh, H.-S. Wong, and K. Saraswat, Proceedings of the University/Government/Industry Microelectronics Symposium, 2006 (unpublished), pp. 47–50.
[11] F. Stern and W. E. Howard, Phys. Rev. **163**, 816 (1967).
[12] M. Kleefstra and G. C. Herman, J. Appl. Phys. **51**, 4923 (1980).
[13] L. Hedin and B. I. Lundqvist, J. Phys. C **4**, 2064 (1971).
[14] S. Jin, M. V. Fischetti, and T.-W. Tang, IEEE Trans. Electron Devices **54**, 2191 (2007).
[15] M. V. Fischetti and S. E. Laux, Phys. Rev. B **48**, 2244 (1993).
[16] S. Jin, M. V. Fischetti, and T.-w. Tang, J. Appl. Phys. **102**, 083715 (2007).
[17] Material parameters taken from: http://www.ioffe.ru/SVA/NSM.
[18] R. Dittrich and W. Schroeder, Solid-State Electron. **43**, 403 (1999).